DOI: 10.21062/mft.2025.025 http://www.journalmt.com

Possibilities of Evaluating the Quality of Products Produced by Directed Energy Deposition Technology

Petr Beneš (0000-0001-5673-0588)[1,2], David Bricín (0000-0002-9354-2751)[2], Denisa Janová (0009-0002-7180-1190)[1]
[1]Faculty of Mechanical Engineering, University of West Bohemia, Univerzitni 2732/8, 301 00, Plzeň. Czech Republic. E-mail: pbenes@fst.zcu.cz; janovad@students.zcu.cz
[2]Centrum výzkumu Řež s.r.o., Morseova 1267/10, 301 00, Plzeň, Czech Republic. E-mail: petr.benes@cvrez.cz; david.bricin@cvrez.cz

It is well known that the porosity of a product can have a negative effect on the mechanical properties of the product. For this reason, its control is very important. Porosity can be assessed by two methods - destructive and nondestructive inspection. However, the identification of very small pores is still very difficult for metallic materials, as the pore size may be below the resolution of most commonly used NDT techniques. In addition, different types of pores may be present in a single part, with one type usually dominating. Proper identification of porosity is essential to estimate the impact on structural properties. For pore assessment, as for other defects, the description of the morphology, distribution and frequency is important. This article deals with the comparison of methods designed to determine the porosity of products that have been manufactured using Laser Directed Energy Deposition – L-DED additive process. The samples were made from AISI 316L stainless steel. The porosity of these samples was assessed using destructive and nondestructive methods. Subsequently, their comparison was made in relation to the detection of different pore sizes. The samples were subsequently subjected to the HIP process (Hot Isostatic Pressing). For these samples, the changes that occurred in the material as a result of this process were subsequently quantified. This process should have a positive effect on improving the quality of the product produced by AM technologies, e.g. by reducing the number and size of pores.

Keywords: AM technology, NDT, material imperfections, HIP process

1 Introduction

Products made with L-DED process are still characterised by the presence of pores despite advances in additive technologies. The formation of pores is the result of gas entrapment or insufficient bonding of the material during the manufacturing process. However, appropriate selection of process parameters can reduce or significantly eliminate the formation of these pores. These parameters include laser power, laser beam scanning speed, and line spacing. By optimally selecting the parameters, component densities of up to 99.99% can be achieved. Low scanning speed leads to high porosity, which is caused by evaporation of low melting temperature elements. However, porosity can also be induced by high scanning speed as a result of insufficient powder melting. Also, low laser power leads to higher porosity, which is attributed to the decrease in wettability. However, the amount and distribution of pores is not always related to printing parameters. It has been found that the powder feed rate can cause a decrease in porosity, unlike scanning speed, where increasing speed usually always results in an increase in product porosity. [1]

Porosity is one of the defects that can be divided according to their dimensions into macroscopic and microscopic. It is believed that 3 main types of pores are formed during AM processes:

- The gas pores are the smallest and have a rounded shape. They are formed by trapping gas that was already present in the metal powder or was trapped during the melting process. It is the most common type of pore formed during AM processes.
- Keyholes pore, these pores resemble a keyhole in shape. These pores are formed as a result of excess input energy. KH pores are relatively large. They are usually circular in the horizontal direction and elongated in the vertical direction.
- Lack of fusion pores, pores created by lack of fusion. These pores are formed by the lack of energy supplied to the powder during the fusion process, leading to its imperfect fusion. LF pores are characterized by shape irregularity and are usually quite large in size.

2 Effect of porosity on the properties of AM products

As with traditionally manufactured materials, porosity strongly influences the mechanical properties of components and structures made with AM technologies. Pores affect the lifetime of a component under static and especially dynamic stresses. For example, in compression tests performed on Ti-6Al-4V alloy deliberately exhibiting high porosity, it was found that the fatigue limit increases with the relative density of the product. [2,3] According to a study that investigated the effect of pores on the mechanical properties of porous Ti-6Al-4V alloy products, it is clear that the geometric morphology of the defect and the porous structure can strongly influence the strength of the material.

In terms of material fatigue, it was found that the value of the fatigue crack propagation stress limit depends on the microscopic pores, while the residual stresses have an effect on the fatigue crack propagation rate. In a material that is absolutely free from the presence of pores or other defects corresponding to the surface, fatigue damage occurs only when cavities caused by the accumulation of dislocations propagate towards the surface. [4] Subsequently, complete destruction of the material occurs. Fatigue damage is influenced by the morphology, localization, location and proportion of internal defects. In imperfect powder fusion, the formation of elongated cavities with sharp corners is the most detrimental type of defect, as it can lead to the accumulation of stresses at the corners of the defect by values that can exceed the applied service load by several times.

According to the research, in which the main characteristics of AM components with increased fatigue life were investigated, the most important factor limiting the lifetime is the large and irregular pores located near the surface. [5] It was also found that gas pores do not have such a significant effect on the fatigue properties of components compared to LF pores. In fact, gas pores are less damaging as they are usually small in size and, most importantly, spherical in shape. [6,7,8]

In general, the negative effects of pores on the mechanical properties of AM products are identical to those of conventionally manufactured products. It is clear from this that the evaluation of the structure in terms of the existence of material defects is highly desirable for the determination of the service life of the product in products manufactured by AM technologies. [9]

3 Post-process elimination of porosity in AM products

Since the elimination of porosity leads to an increase in product quality, there are many techniques to reduce or completely eliminate the presence of pores in AM products. [10] The HIP (Hot Isostatic Pressing) method is one of the most effective methods for achieving porosity reduction in a product. When this method is applied, the internal porosity is closed. This method is very simple in principle. The product is placed in a pressure vessel where very high pressure is applied to the product under elevated temperature conditions. The pressure is usually implemented by an inert gas. The pressure and temperature causes the collapse, diffusion of pores or other volume defects present in the body. The consequence of the HIP process is therefore a significant reduction in porosity, which leads to an increase in the density of the component. This treatment therefore improves the overall mechanical properties of the material, particularly fatigue life. HIP technology as a post-process treatment is generally not limited by the initial state of the product, the way it is manufactured, so that this technology can be applied to all types of products. Despite the undeniable advantages, the HIP technique also has some disadvantages. For example, it may not be effective for parts with high structural and shape complexity. At high temperature, the HIP process can cause significant grain coarsening, which can lead to a reduction in static strength. Also, it must be taken into account that, during operation, the pores usually enlarge and shrink during the HIP process.

Another post-processing option to reduce porosity is the so-called Ultrasonic Peening Treatment (UPT). This method uses low-amplitude high-frequency oscillations of the tip acting on the surface of the manufactured part. This mechanism induces plastic deformation of the surface, effectively sealing material defects including pores. A similar principle is used in the post-processing of the so-called Laser Shot Peening (LSP) technique, where laser pulse-mediated shock waves are applied to the material surface.

4 Evaluation of porosity in AM products

Different methods can be used to determine porosity. These methods are possible divided into destructive (DT) and nondestructive (NDT). These techniques can be further subdivided into methods designed to determine the presence of open pores, i.e., pores interacting with the surface (surface defects), and closed pores, which are located close to or at greater distances from the surface (volume defects). The presence of surface defects by NDT methods can be evaluated visually or using penetrant testing and ultrasound. The presence of subsurface defects can be assessed using both ultrasound and, for example, X-ray radiography tests. In destructive evaluation, a sample is then taken and analysed by light and electron microscopy. This provides an overview of the pores' distribution and shape and, through local microanalysis, the chemical and phase composition of the

surrounding area. The above methods differ in their discriminating ability, i.e. the ability to detect structural defects of a certain size and quantity, which is determined by the physical nature of each method and depends, for example, on the chemical and phase composition of the material being analysed.

This paper aimed to compare common NDT methods in terms of their ability to detect pores in as-printed and HIP heat-treated AISI316L austenitic steel produced by the L-DED process. The NDT results were supported and verified by porosity analysis on metallographic samples (DT test).

5 Material and methods

The material used for printing was AISI 316L steel. A total of 3 samples were produced with dimensions of approximately 33 x 33 x 18 mm (length x width x height). The samples were produced by the L-DED process using the InSSTek MX-600 equipment with parameters shown in Table 1. Orientation of the sample during its production relative to the coordinate system is shown in the Figure 1.

Some of samples were subsequently subjected to the HIP process after the performed NDT analyses. The main parameters of the HIP process are shown in Table 2. Further experiments were subsequently performed on this sample to determine any changes in material structure that were induced by the HIP process. It was hypothesized that the HIP process would reduce or eliminate the amount and size of pores present.

Tab. 1 *Printing parameters*

Parameter	Value
Dipping head	SDM1600
Laser diameter	1 600 μm
Layer height	600 μm
Distance of individual laser paths from each other (hatch distance)	1 100 μm
Amount of powder	5.6 g/min
Coaxial gas	10 l/min
Protective gas	10 l/min
Carrier gas for powder	2.5 l/min
Press strategy	ZigZag CFC+CF
Laser power	DMT approx. 1 000 W
Printing time	50 min

Tab. 2 *HIP process parameters*

Temperature	1150°C
Pressure	100 MPa
Atmosphere	Argon
Cooling rate up to 800 °C	6.6°C/s

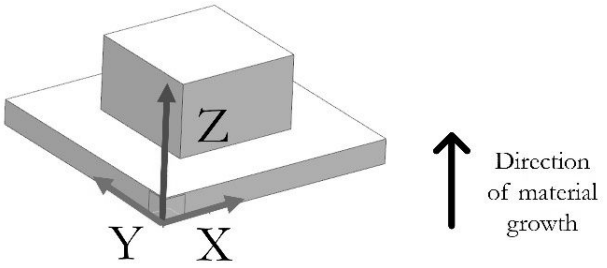

Fig. 1 *Orientation of sample during its production*

NDT analysis before and after HIP process was done using radiography test, penetrant test and ultrasonic test. Surface of specimens was grinded and polished before NDT testing to get suitable surface roughness for each used NDT technique.

The penetrant test was performed to determine the surface porosity. The standard testing procedure as used for NDT techniques was applied.

The radiography examination was performed using an industrial X-ray system with a DXR250U-W digital detector. This system has a minimum resolution of 200 μm detail. To increase the contrast of the X-ray images, Cu foil was used during the exposures. Different image filtering was used to improve the visibility of possible material defects.

The ultrasonic test was performed with an industrial defectoscope Olympus Epoch 1000i. The measurement was carried out by Pulse - Echo method (PEUT) and Phased Array method (PAUT) (Olympus 5L16-A10 probe used). The ultrasonic test was performed both in the direction of layer growth and in the direction perpendicular to the direction of layer growth. This method required sample surface preparation, which consisted of grinding all sample surfaces. In the case of the Phased Array method, S-scan and linear B-scan were used. In the case of the Pulse-Echo method, only the A-scan was recorded.

The ultrasonic test also evaluated the attenuation of the ultrasonic signal, as the attenuation value is strongly influenced by the porosity of the material. The attenuation measurements were performed in the perpendicular direction (xy direction) and in the direction (xz direction) of growth of the individual material layers. To increase the accuracy of the measurements, different types of ultrasonic probes were used, namely longitudinal and transverse wave probes of different frequencies (operating frequencies of 1,4,5,10 MHz were used).

Helium pycnometry was performed with Pycnomatic ATC instruments. For this measurement, an Ohaus Discovery DV214C analytical balance was used to measure the weight of the samples.

Metallography analysis was done in the direction of layer growth (X-Z direction) for all samples (i.e. sample processed by L-DED and sample further heat treated by HIP) and X-Y direction. Analysis was done

after specimen surface preparation by grinding, polishing, and etching by Kallings 2 etchant. Porosity and structure analysis was done using a light microscope CarlZeiss Observer Z1m and scanning electron microscope Tescan Mira 3 in combination with local analysis of chemical composition by EDS measurement. To statistically determine the average pore area distribution, 10 images were taken at 100x magnification for each sample. The average pore area was evaluated using Zeiss ZenCore software.

6 Result and discussion

The penetrant test after samples´ processing by L-DED revealed the presence of isolated pores in two samples (samples 2,3). That indicates really low surface porosity of specimens, or open type of porosity. That result thus indicates if there is the presence of porosity it is a closed type which can be eliminated by the HIP process. No detectable defect was found in any of the samples before HIP process by the radiography test. This implies that any indications are smaller in size than the resolution of the detector, i.e. less than 200 μm.

As can be seen from Table 3 no significant differences in the ultrasonic wave attenuation in the transverse and longitudinal directions of the sample were observed. The slightly larger scatter of values for the 1 MHz transverse wave in samples 2 and 3 is due to the small size of the sample to be measured and the size of the ultrasonic wave wavelength, where low frequency measurements are not sufficiently accurate for such small samples. Ultrasonic testing that indicates that there was no defect in L-DED or HIP processed specimens, or the size of the defect was below the resolution of this method.

Metallography analysis against NDT methods show that in volume of specimens is possible inidicate some porosity and inclusions, see Figure 2 and Table 4.

Tab. 3 *Ultrasonic wave attenuations*

	α [dB/mm]	1 MHz transverse wave	5 MHz transverse wave	4 MHz longitudinal wave	10 MHz longitudinal wave
Sample 1	Longitudinal direction - xy	0.0305	0.0355	0.0352	0.0358
	Transverse direction - xz	0.0308	0.0344	0.0364	0.0355
Sample 2	Longitudinal direction - xy	0.0319	0.0352	0.0343	0.0367
	Transverse direction - xz	0.0277	0.0355	0.0364	0.0354
Sample 3	Longitudinal direction - xy	0.0315	0.0347	0.0347	0.0355
	Transverse direction - xz	0.0278	0.0347	0.0360	0.0362
After HIP process	Longitudinal direction - xy	N/A	0.0347	N/A	0.0370
	Transverse direction - xz	N/A	0.0351	N/A	0.362

Despite the fact that the observed porosity values of the individual samples differ from each other (e.g. the porosity of sample 2 is approximately 5 times greater than that of sample 1), see Table 4, it is evident from the measured values that the proportion of defects or pores is very low in all samples and the percentage of pores does not exceed 1% in any sample. The observed magnitude of the porosity of the samples is consistent with the measured values of the sample densities measured by Helium pycnometry, see Table 4. As can be seen from the comparison of pore and inclusions sizes and frequencies in different section directions for sample 3 (Figure 2), a higher proportion of larger pores was found in the section made in the direction perpendicular to the layer growth direction compared to the layer growth direction. Pores and inclusions in the size interval (1;5⟩ μm were the most frequent. In this image resolution is hard to distinguish between pore or inclusion which may have similar portrayals. The second most abundant pores were in the size interval (5;10⟩ μm in the case of the section in the direction of layer growth, and in the case of the section perpendicular to the direction of layer growth, they were in the size interval (10;50⟩ μm. For sample 3, one pore of size 282 μm was detected. From the measured values of the pore sizes, it is clear that the sizes of these indications are

below the detectable level of the conventional radiography and ultrasonic tests used. Such small pores can be detected by penetrant testing, provided that the pore is sufficiently large to trap a sufficient amount of penetrant and, of course, must also correspond to the surface.

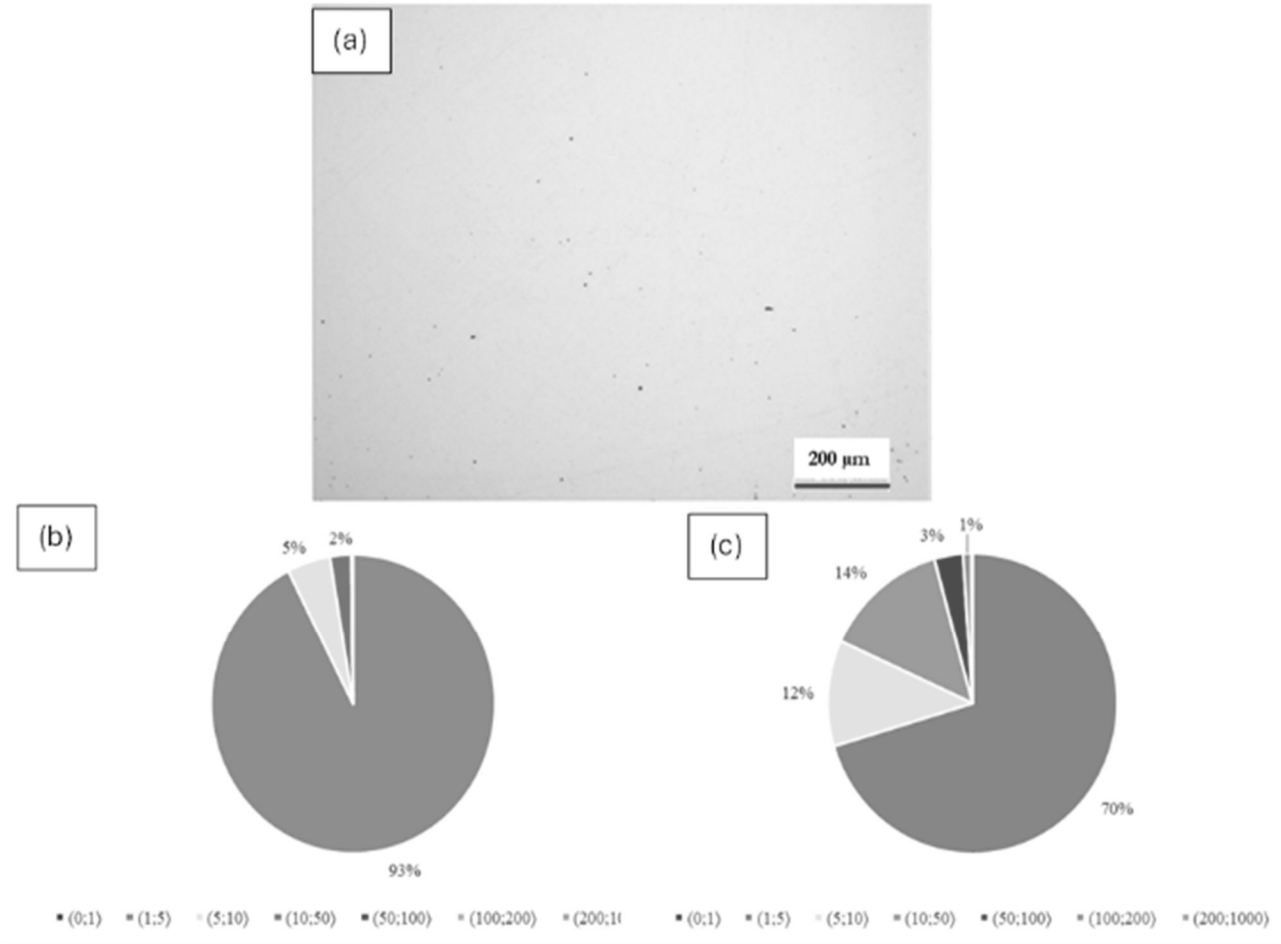

Fig. 2 *(a) Metallographic cross-section of the sample (cut in the direction of sample growth xz) with pores marked; (b) Percentage distribution of pore size in µm in the direction of layer growth (xz); (c) Percentage distribution of pore size in µm in the direction perpendicular to the growth of the layers*

Tab. 4 *Percentage of defects in the cut area, cut in the direction of layer growth xz and values of densities measured with pycnometer for L-DED specimens*

	Sample 1	Sample 2	Sample 3
Sample density [kg/m³]	7 914.56 ± 0.01 %	7 916.04 ± 0.01 %	7 922.94 ± 0.01 %
Percentage of defects in the cut area (layer growth direction xz) (L-DED) [%]	0.14 ± 0.02	0.65 ± 0.08	0.36 ± 0.04

A more detailed description of the pores and inclusions in the samples' structure after L-DED and HIP processing was done using a scanning electron microscope in combination with local EDS chemical composition analysis. It was possible to identify chromium and mangenese rich oxide nanoparticles in the structure of the samples after L-DED and HIP processing, see Figure 3(a). The size of these particles was around 386 ± 107 nm for the sample after L-DED processing and around 404 ± 85 nm for the samples after HIP processing. The concentration of these particles in the evaluated area was around 0.54 ± 0.22 % for the L-DED samples and around 0.52 ± 0.1 % for the HIP sample. The above results show that the oxide inclusions coarsened during HIP processing. This coarsing of the particles could have occurred for several reasons. One of the possible reasons is too high temperature and long soaking time at this temperature. It is also possible that particle microstructure was too fine grained, which increases the susceptibility to the thickening of some particles.

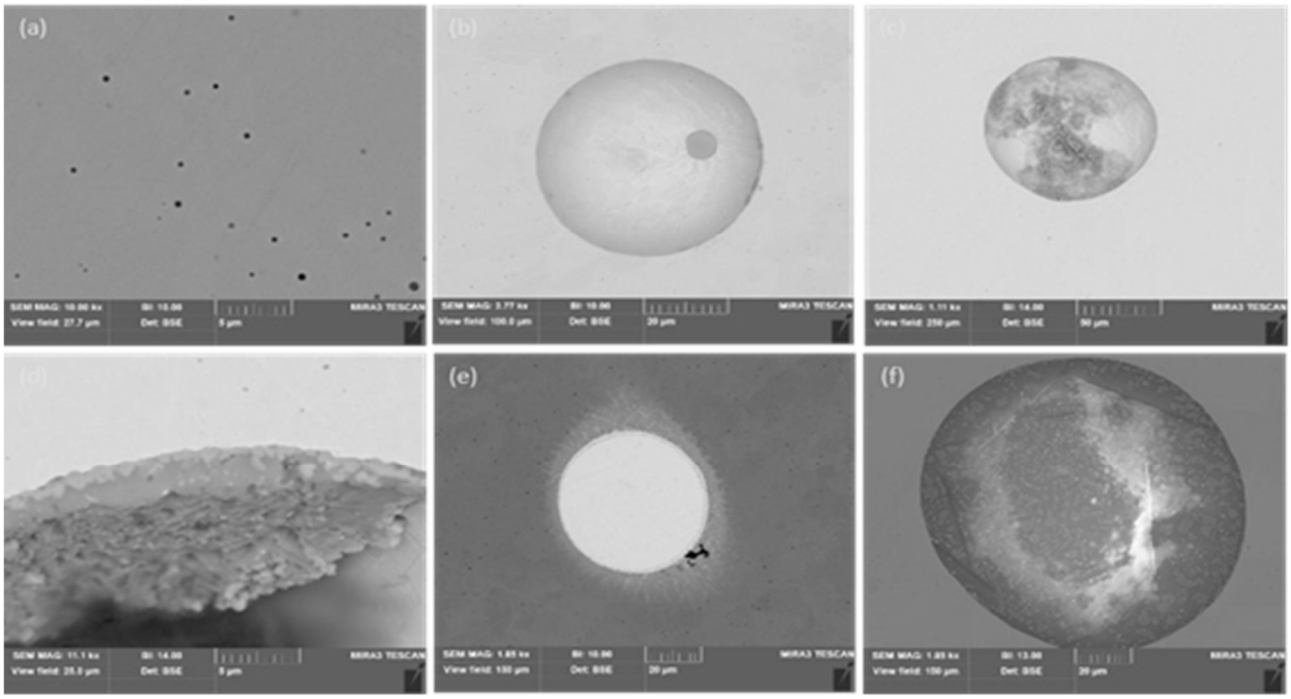

Fig. 3 *Pores structure; (a) (Mn,Cr)O submicron's oxide inclusions - chemical analysis of these oxide particles was performed see Figure 4(a); (b) Pore volume with small surface contamination; (c) Pore volume with presence of oxide film surface contamination; (d) Detail of internal surface oxide film contamination; (e) Pore volume filled with tungsten particle inclusion contaminant; (f) Pore volume filled with complex oxide contaminant based on Al*

A minority of the sample structure consisted of pores and oxide particle of circular cross-section up to 160 μm in size. Some types of these inhomogenities could be identified in the sample structure after L-DED and HIP processing, see Figure 3(b-f). For the L-DED samples, these pores could be divided into two categories, namely pores without the presence of inclusions and pores with the volume filled with inclusions either partially by oxide or almost completely.

These inclusions could be divided into two categories as follows:

- Inclusions formed during the melting of the processed powder, these consisted primarily of Mn and Cr oxides, see Figure 4(a).
- Inclusions of contaminants, were either complex oxides of diverse types of non-ferrous metals, e.g. Al or Zr, or tungsten carbide particles, see Figures 4(b-c).

The presence of pores was not observed in the sample after HIP treatment. HIP therefore resulted in their closure. Oxide inclusions of circular cross-section up to 160 μm in size were possible to observed in both types of specimens L-DED and HIP treated. From that is possible to conclude that HIP doesn't led to their reduction and these particles will play important role for fatigue life of specimens.

Measurements were made by destructive and non-destructive methods to assess and quantify defects in products that were manufactured using additive DED technology. It was found that the conventional methods of ultrasonic testing and radiography test could not detect the defects present, as the dimensions of the defects (pores) present in the prints were below the resolving power of the detectability of these methods. The only nondestructive method that has detected and quantified the presence of internal defects is He pycnometry. Using this method it is possible to quantify the number of internal defects in the material. The penetrant test was able to detect larger surface defects, however, its applicability is obviously only for the surface area of the sample. Thus, in the case of AM technology products, it is only possible to reliably detect and quantify the extent of internal defects using light or other microscopy, particularly with the aid of appropriate image analysis.

The analyses carried out have shown that at present, products produced by AM L-DED technology are comparable or even better than products produced by other traditional technologies in terms of internal quality. For example, in the production of high-pressure die-casting components, porosity is typically in the order of tens of percent. Experiments have also shown that the samples examined do not exhibit any structural anisotropy. This points to the fact that it is now possible to produce a product by AM L-DED technology that can replace products produced by other technologies. Any porosity, even if minimal, in products produced by AM technologies can be effectively reduced by subsequent additional processes, e.g. by HIP technologies.

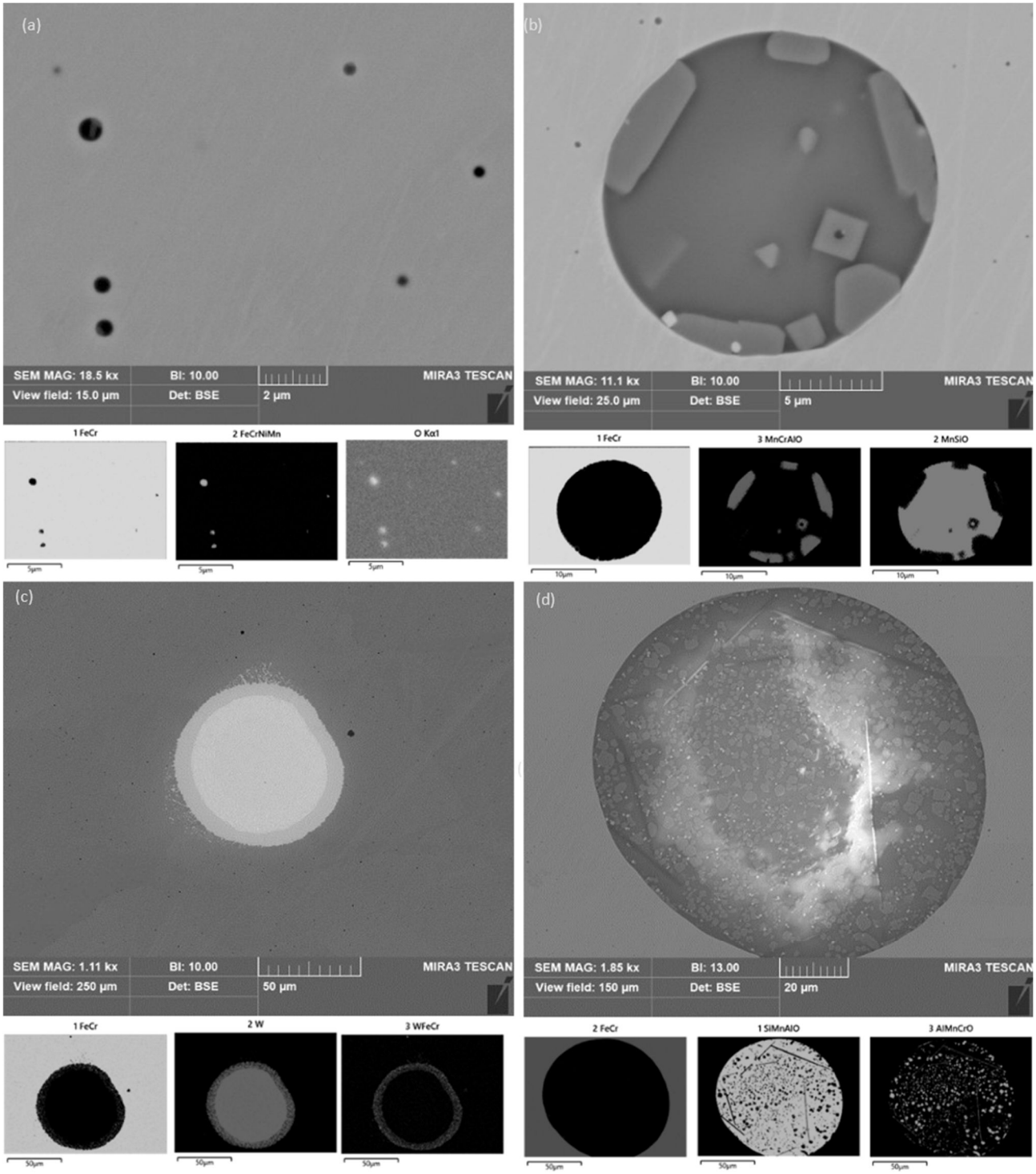

Fig. 4 *Pores contaminants EDS analysis results (maps of chemical phase analysis); (a-b) Inclusions formed from processed powder. Inclusions formed from processed powder; (c-d) Inclusions of contaminants based on Al, Zr and W*

7 Conslusion

This study aimed to compare basic NTD techniques used for analysing of defect presence in the material in the case of L-DED and further HIP-treated specimens made of AISI316L steel. NDT results showed that there was no porosity in specimen volume, i.e. porosity was in almost all cases below the resolution of used NDT methods. Microstructure analysis using LOM and SEM against NDT showed that in specimen volume is possible to evaluate porosity. The porosity level was low and was below 0.5 % for all types of specimens. The maximum size of pores was about 160 um. After the HIP process pores were not observed in the volume of specimens. It was possible to find just oxide inclusions with sizes like pores. These oxide inclusions were created during the L-DED process from molten powder and non-ferrous inclusions.

From the above experimental program it is clear that the L-DED technique can produce a product containing minimal material defects, which can also be effectively eliminated by post-processing procedures, e.g. the HIP process. Manufacturing defects of AM products are generally below the detection limits of most commonly used NDT techniques.

Acknowledgement

The presented results were obtained thanks to the collaboration with Comtes FHT a.s. The presented work has been realized within Institutional Support by the Ministry of Industry and Trade of the Czech Republic. The presented results were obtained using the CICRR infrastructure, which is financially supported by the Ministry of Education, Youth and Sports - project LM2023041.

References

[1] MORALES, CINDY & MERLIN, MATTIA & FORTINI, ANNALISA & FORTUNATO, ALESSANDRO. (2023). Direct Energy Depositions of a 17-4 PH Stainless Steel: Geometrical and Microstructural Characterizations. *Coatings*.

[2] S.J. LI, L.E. MURR, X.Y. CHENG, Z.B. ZHANG, Y.L. HAO, R. YANG, F. MEDINA, R.B. WICKER, Compression fatigue behavior of Ti–6Al–4V mesh arrays fabricated by electron beam melting, *Acta Materialia*, Volume 60, Issue 3, 2012, Pages 793-802, ISSN 1359-6454, https://doi.org/10.1016/j.actamat.2011.10.051.

[3] TIAN W, WANG W, WANG Y, ZHANG S. Study on Multi-Objective Optimization of Milling Process of Powder Metallurgy Titanium Aluminum Alloys. *Manufacturing Technology*. 2024;24(4):652-667. doi: 10.21062/mft.2024.064.

[4] S. LEUDERS, M. THÖNE, A. RIEMER, T. NIENDORF, T. TRÖSTER, H.A. RICHARD, H.J. MAIER, On the mechanical behaviour of titanium alloy TiAl6V4 manufactured by selective laser melting: Fatigue resistance and crack growth performance, *International Journal of Fatigue*, Volume 48, 2013, Pages 300-307, ISSN 0142-1123, https://doi.org/10.1016/j.ijfatigue.2012.11.011.

[5] AREF YADOLLAHI, NIMA SHAMSAEI, Additive manufacturing of fatigue resistant materials: Challenges and opportunities, *International Journal of Fatigu*e, Volume 98, 2017, Pages 14-31, ISSN 0142-1123, https://doi.org/10.1016/j.ijfatigue.2017.01.001.

[6] AREF YADOLLAHI, NIMA SHAMSAEI, Additive manufacturing of fatigue resistant materials: Challenges and opportunities, *International Journal of Fatigue*, Volume 98, 2017, Pages 14-31, ISSN 0142-1123, https://doi.org/10.1016/j.ijfatigue.2017.01.001.

[7] T. DEBROY, H.L. WEI, J.S. ZUBACK, T. MUKHERJEE, J.W. ELMER, J.O. MILEWSKI, A.M. BEESE, A. WILSON-HEID, A. DE, W. ZHANG, Additive manufacturing of metallic components – Process, structure and properties, *Progress in Materials Science*, Volume 92, 2018, Pages 112-224, ISSN 0079-6425, https://doi.org/10.1016/j.pmatsci.2017.10.001.

[8] SHAFAQAT SIDDIQUE, MUHAMMAD IMRAN, ERIC WYCISK, CLAUS EMMELMANN, FRANK WALTHER, Influence of process-induced microstructure and imperfections on mechanical properties of AlSi12 processed by selective laser melting, *Journal of Materials Processing Technology*, Volume 221, 2015, Pages 205-213, ISSN 0924-0136, https://doi.org/10.1016/j.jmatprotec.2015.02.023.

[9] BURDOVÁ K, JIRKOVÁ H, KUČEROVÁ L, ZETKOVÁ I, MACH J. Effects of Heat Treatment on Additively Manufactured 316L Stainless Steel. *Manufacturing Technology*. 2022;22(3):261-266. doi: 10.21062/mft.2022.042.

[10] BECHNÝ V, MATUŠ M, JOCH R, DRBÚL M, CZÁN A, ŠAJGALÍK M, NOVÝ F. Influence of the Orientation of Parts Produced by Additive Manufacturing on Mechanical Properties. *Manufacturing Technology*. 2024;24(1):2-8. doi: 10.21062/mft.2024.021.